

Triangular Pore Formation in Highly Doped n-type 4H SiC

Y. Shishkin, W. J. Choyke, and R. P. Devaty*

Department of Physics and Astronomy, University of Pittsburgh, Pittsburgh, PA 15260, USA

Keywords: porous, photoelectrochemical, etching

Abstract. Our study of photoassisted electrochemical etching of highly doped n-type 4H SiC shows that the anodization proceeds anisotropically. As a result, a triangular-channel porous structure is formed independent of the direction of the external electric field applied to the sample. It is proposed that the observed pore morphology is due to differences in oxidation rates of the crystallographic planes terminated with silicon and carbon atoms.

Introduction

Since Shor and colleagues [1] demonstrated that porous silicon carbide could be fabricated by anodizing single-crystal n-type (0001) 6H SiC wafers in aqueous HF there have been a number of reports on the subject. Porous SiC is a promising material for applications including epitaxial film growth on porous substrates [2] and the study of electrically active centers near the SiC/SiO₂ interface by Electron Paramagnetic Resonance [3]. Projects such as protein dialysis, bone tissue engineering, and fuel cell fabrication involving the use of porous self-supporting SiC films as well as porous layers on substrates are being actively pursued. It is likely that a variety of porous morphologies are needed to satisfy different applications. Porous structures which can be obtained under the photoassisted as well as the dark-mode conditions in SiC have been reported elsewhere [4]. The possibility of a number of fabricated morphologies indicates that anisotropy exists in the pore propagation in hexagonal SiC. Here, we focus on a triangular pore morphology obtained in highly doped n-type crystals by photoelectrochemical etching under low voltage and/or current density conditions. We concentrate on our etching experiments carried out not only on the basal Si-face but also the C-face and the non-basal a- and p-faces of n-type 4H SiC. We explain the observed anisotropy in the pore morphology using both crystallographic properties of the hexagonal 4H SiC lattice and a model for the semiconductor/electrolyte interface. The latter is based on the semiconductor space charge model as in a Schottky semiconductor/metal junction.

Experimental

The 4H SiC samples used in this study are nitrogen-doped at $5 \cdot 10^{18} \text{ cm}^{-3}$ to $7 \cdot 10^{18} \text{ cm}^{-3}$. The etching is performed in aqueous 5% HF (measured by weight) solution mixed with ethanol in the ratio HF:ethanol = 1:1. The front of the sample surface is illuminated by UV light during the experiment. The UV source is a 350W mercury arc with filters to restrict the spectrum to the wavelength interval from 2967 to 4045 Å. The UV power density is about 160 mW/cm² as measured by a thermopile-type power meter. The photoelectrochemical etching is conducted in a standard three-electrode electrochemical cell where a SiC crystal serves as the working electrode, a platinum plate as the counter electrode, and a saturated calomel electrode as a reference for the potential. The electrical current through the sample is controlled with a PAR 263A potentiostat/galvanostat. The etching is conducted anodically corresponding to the reverse bias regime. In the potentiostatic regime the bias is set at three volts to minimize the dielectric breakdown effects. Galvanostatic etching is performed using current densities up to 5 mA/cm² at biases which do not exceed three volts. After anodization, samples are carefully removed from the bath and cleaned in acetone to prepare them for plan-view and cross-sectional SEM imaging performed on a Philips XL 30 FEG electron microscope.

* corresponding author, e-mail: devaty@pitt.edu

Results and Discussion

The cross-sectional SEM image in Figure 1 shows the triangular porous morphology obtained in 8° off-cut (0001) 4H SiC samples ($n \sim 6 \cdot 10^{18} \text{ cm}^{-3}$) made by UV-photoassisted electrochemical etching at a 3Volt reverse bias. The current density at this bias did not exceed 5 mA/cm^2 . The particular surface exposed to the imaging by fracturing the sample is the $(1\bar{1}00)$ plane. The morphology can be described as a stack of roughly planar layers perforated by rows of approximately equilateral triangles. The average distance between each individual pore as well as the neighboring layers varies in the range of 35 to 40 nm. The triangular pores appear roughly equidistantly placed and tend to propagate normal to the [0001] direction suggesting that the basal (0001) plane possesses an etch-stop character. The tip of each triangle always points toward the [0001] direction.

Processing the front surface by Reactive Ion Etching (RIE) with SF_6 gas reveals that the porous network has channeled structure. Figure 2 shows how a vicinal basal plane appears with roughly two microns of the porous film removed. The channels branch out, wriggle, and occasionally intersect each other. The slight preference for channel propagation along $\langle 1\bar{2}10 \rangle$ and its equivalent directions exhibited on Figure 2 by the arrows suggests that the $(1\bar{2}10)$ plane is relatively susceptible to HF electrolytic attack.

When similar conditions of photoassisted electrochemical etching are applied to the vicinal $(000\bar{1})$ C-face of 4H SiC n-type samples, the layered planar pore structure is not observed. Figure 3 shows the corresponding morphology in cross-section. The RIE removal of the top of the porous film reveals no channels but rather rounded pits on the surface (not shown). Consequently, the pores in the C-face crystals are formed in the shape of intricately connected cones. In spite of the differences, the average pore size and the size of the interpore spacing are the same as compared to the etched vicinal (0001) Si-face. Moreover, the direction toward which every cone points is [0001].

Anodization is also done on non-basal $(1\bar{1}00)$ and $(1\bar{2}10)$ faces, also called the p- and the a-face, respectively. The plan view SEM images show triangles on the etched surfaces indicating an anodization anisotropy. After being fractured, the samples are subjected to cross-sectional SEM analysis. The images reveal that the size and the shape of the triangular pores and their general planar layout are preserved as compared to the vicinal (0001) Si-face samples (see Figure 4). For example, when a cross-sectional image of a $(1\bar{1}00)$ sample (the surface presented in the picture is the $(1\bar{2}10)$ -face) is rotated clockwise it resembles the picture shown in Figure 1. The similarity is

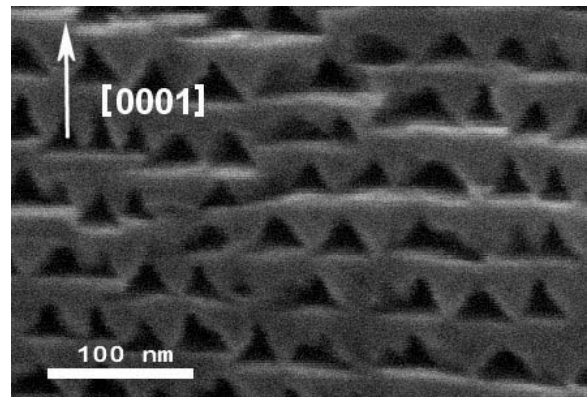


Figure 1. Cross-sectional SEM image of a porous n-type highly doped 4H SiC Si-face sample photoelectrochemically etched at 5 mA/cm^2 .

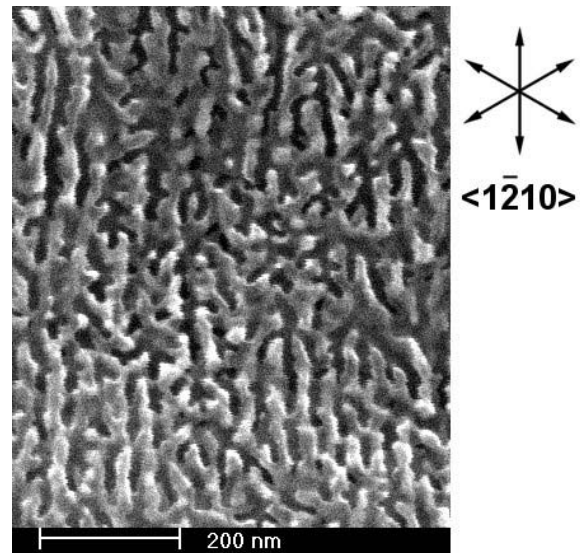


Figure 2. Plan-view SEM image of a porous vicinal 4H SiC sample RIE-etched to remove about $2 \mu\text{m}$ from the top of the film. The exposed channels are seen to propagate preferentially along the $\langle 1\bar{2}10 \rangle$ directions.

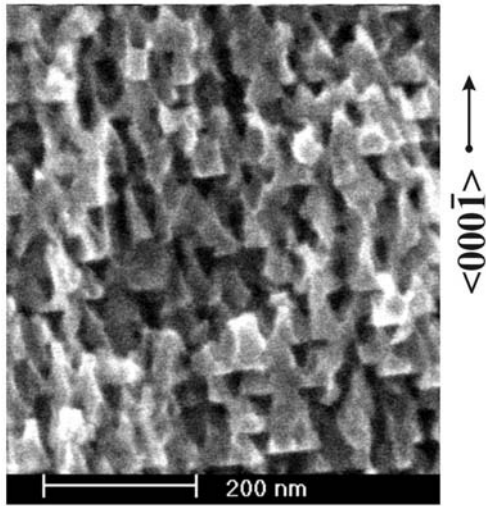


Figure 3. Cross-sectional SEM image of a porous n-type highly doped 4H SiC C-face photoelectrochemically etched sample. The planarity characteristic to the etched vicinal (0001) samples is not observed.

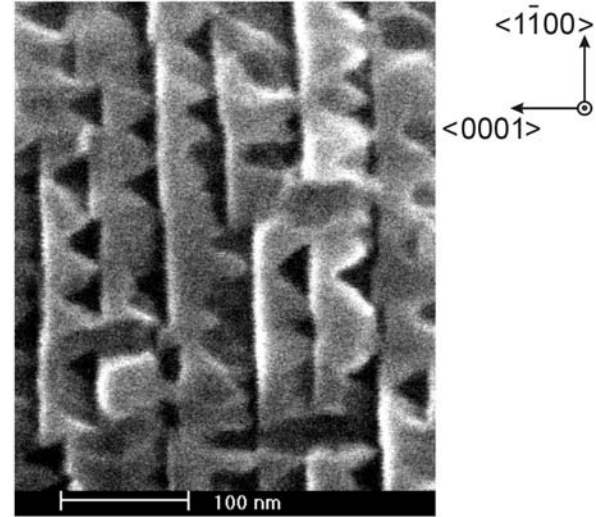


Figure 4. Cross-sectional SEM image of a porous n-type highly doped 4H SiC (1-100) sample. The particular surface exposed for the imaging is a $\{11\bar{2}0\}$ face. When this picture is rotated 90° clockwise it resembles the cross-sectional image of a vicinal (0001) sample.

striking despite the fact that during etching the electric field is applied parallel to the basal plane and consequently perpendicular to the field applied for etching the (0001) Si-face samples. Even though the structures obtained by etching $(1\bar{1}00)$ and $(1\bar{2}10)$ surfaces are very similar, we observe a difference in the etch rates defined as the thickness of a porous layer etched per unit time. This rate is a factor of two larger for the $(1\bar{2}10)$ plane than for the $(1\bar{1}00)$ plane under identical etching conditions. This fact supports our observation, deduced from Figure 2, that the $(1\bar{2}10)$ surface is preferred under the electrolytic action. Qualitatively this can be explained by the differences in respective surface energies. In hexagonal polytypes of SiC, $\{1\bar{2}10\}$ surfaces have a higher surface energy, and thus are less stable, than the $\{1\bar{1}00\}$ surfaces [5].

Using the published differences of the oxidation rates of the (0001) Si- and $(000\bar{1})$ C-faces [6] we propose a qualitative model for the formation of the triangular pore morphology. The oxidation of a C-terminated surface proceeds much faster than the oxidation of a Si-face. Since pore formation is an oxidation process followed by immediate dissolution of the formed oxide, a “slow-oxidizing” silicon-terminated surface can therefore be considered as an etch stop. Figure 5 shows the $(1\bar{2}10)$ plane. The zigzagged solid lines which connect white dots (silicon atoms) represent the surfaces associated with the $(\bar{1}10\bar{2})$ and $(1\bar{1}0\bar{2})$ planes. These planes correspond to the walls tilted at about 60 degrees relative to the basal plane Si-face that comprises the base of the formed triangle. The $(\bar{1}10\bar{2})$ and $(1\bar{1}0\bar{2})$ surfaces are terminated with silicon atoms, although the density of the dangling bonds is one and a half times larger than on the (0001) unreconstructed surface. We believe such silicon termination makes the $\{1\bar{1}0\bar{2}\}$ planes withstand the electrolytic attack under anodization conditions better than any other planes, except (0001). Therefore, we suggest that two sides of each triangle are made from surfaces corresponding to the $\{1\bar{1}0\bar{2}\}$ family of planes. This fact plus preferential pore propagation along the $\langle 1\bar{2}10 \rangle$ directions create the necessary environment for the observed triangular pore shape and the observed channels.

In order to explain the typical pore size distribution (i.e. the average triangular channel dimensions seen in cross-section), let us consider a SiC/electrolyte interface as analogous to a

Schottky semiconductor/metal junction. Such an approach is justified in sufficiently concentrated solutions for non-degenerate semiconductors. A space charge (depletion) region (SCR) is assumed near the surface of the semiconductor where almost all the applied potential is dropped [7]. By estimating the width of the SCR, a rough theoretical estimate of the average dimensions of the triangular pores can be obtained. The depletion layer width is obtained by solving Poisson's equation and is given by $L = \sqrt{2\epsilon\epsilon_0\phi_{sc}/en}$, where ϕ_{sc} is the potential drop in the SCR of the semiconductor and ϵ is the static dielectric constant [7]. For a carrier concentration $n \sim 6 \cdot 10^{18} \text{ cm}^{-3}$ L is estimated to be about 30 nm in SiC with a 3Volt bias. At such high doping the rigorous calculation of L requires the use of Fermi-Dirac statistics. Still, the estimated value of 30 nm is roughly in agreement with the average distance between triangles as well as the average planar layer thickness observed by SEM imaging. Hence we believe that the growth of the porous matrix is governed by a self-regulation of the pore nucleation sites based on the assumption that the interpore spacing is depleted of charge carriers and, consequently, resistant to further electrolytic attack [8].

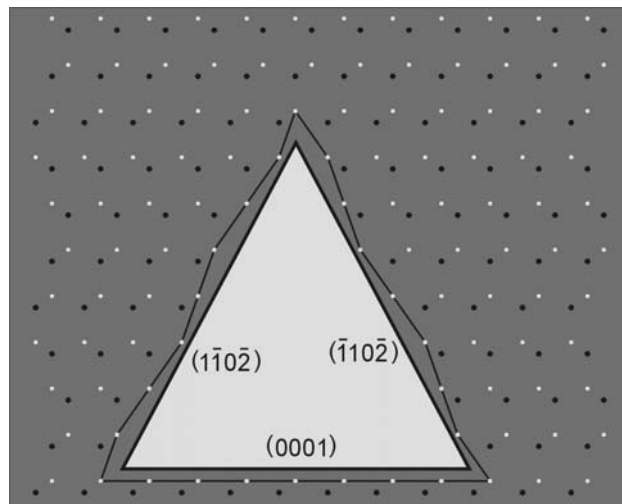


Figure 5. A schematic of the projection of the 4H SiC crystal lattice as viewed from a $[1\bar{2}10]$ direction. The triangle represents a cross-section of a pore channel typically seen in photoelectrochemically etched highly doped 4H SiC. The planes comprising the walls of the triangular channel are indicated. Light dots represent Si atoms, black – C atoms.

Conclusion

The photoelectrochemical etching of (0001) , $\{1\bar{1}00\}$, and $\{1\bar{2}10\}$ surfaces of highly doped 4H SiC has been studied. We find that at a reverse bias comparable to the bandgap the shape and the size of the pores and the overall macroscopic porous structure are the same indicating independence of the direction of the applied electric field. A qualitative model describing the crystallographic aspects of the pore propagation is proposed. This model is used to characterize the observed triangular channel pore morphology. The observed pore dimensions are explained in terms of the depletion width approximation based on an analogy with a Schottky semiconductor/metal interface.

Acknowledgment

We wish to acknowledge the DURINT Program (ONR Grant –N00014-01-1-0715) for supporting this research. We also thank A. Sagar and Y. Ke for help with RIE processing.

- [1] J.S. Shor, I. Grimberg, B.-Z. Weiss, and A.D. Kurtz, *Appl. Phys. Lett.* 62 (1993), p. 2836
- [2] M. Mynbaeva, S.E. Sadow, G. Melnychuk, I. Nikitina, M. Scheglov, A. Sitnikova, N. Kuznetsov, K. Mynbaev, and V. Dmitriev, *Appl. Phys. Lett.* 78 (2001), p. 117
- [3] H.J. von Bardeleben, J.L. Cantin, M. Mynbaeva, S.E. Sadow, Y. Shishkin, R.P. Devaty, and W.J. Choyke, *Electrochem. Soc. Proc.* Vol. 2003-02, pp. 39-51; also this conference
- [4] S. Bai, *et al.*, *Mat. Res. Soc. Symp. Proc.* Vol. 742 (2003), p. 151
- [5] E. Rauls, J. Elsner, R. Gutierrez, and Th. Frauenheim, *Solid State Commun.* 111 (1999), p. 459
- [6] L. Muelhoff, W.J. Choyke, M.J. Bozack, and J.T. Yates, Jr., *J. Appl. Phys.* 60 (1986), p. 2558
- [7] Yu.V. Pleskov and Yu.Ya. Gurevich, *Semiconductor Photoelectrochemistry* (Counsultants Bureau, New York, 1986)
- [8] A.O. Konstantinov, C.I. Harris, and E. Janzen, *Appl. Phys. Lett.* 65 (1994), p. 2699